

Contrast enhancement for improved blood vessels retinal segmentation using top-hat transformation and otsu thresholding



Muhammad Arhami ^{a,1}, Anita Desiani ^{b,2,*}, Sugandi Yahdin ^{b,3}, Ajeng Islamia Putri ^{b,4}, Rifkie Primartha ^{c,5}, Husaini Husaini ^{d,6}

^a Informatics Engineering Departement, Politeknik Negeri Lhokseumawe, Lhokseumawe, Indonesia

^b Mathematics Departement, Mathematics and Natural Science Faculty, Universitas Sriwijaya, Inderalaya, Indonesia

^c Informatics Engineering Departement, Computer Science Faculty, Universitas Sriwijaya, Inderalaya, Indonesia

^d Network Computer Engineering Departement, Politeknik Negeri Lhokseumawe, Lhokseumawe, Indonesia

¹ muhammad.arhami@pnl.ac.id; ² anita.desiani@unsri.ac.id; ³ sugandi@unsri.ac.id; ⁴ 08011381621046@unsri.ac.id;

⁵ rifkie@ilkom.unsri.ac.id; ⁶ husaini@pnl.ac.id

* corresponding author

ARTICLE INFO

Article history

Received February 2, 2022

Revised April 17, 2022

Accepted May 13, 2022

Available online July 31, 2022

Keywords

Segmentation

Image Enhancement

Otsu Thresholding

CLAHE

Top-Hat Transformation

Blood Vessels

Retina

ABSTRACT

Diabetic Retinopathy is a effect of diabetes. It results abnormalities in the retinal blood vessels. The abnormalities can cause blurry vision and blindness. Automatic retinal blood vessels segmentation on retinal image can detect abnormalities in these blood vessels, actually resulting in faster and more accurate segmentation results. The paper proposed an automatic blood vessel segmentation method that combined Otsu Thresholding with image enhancement techniques. In image enhancement, it combined CLAHE with Top-hat transformation to improve image quality. The study used DRIVE dataset that provided retinal image data. The image data in dataset was generated by the fundus camera. The CLAHE and Top-hat transformation methods were applied to rise the contrast and reduce noise on the image. The images that had good quality could help the segmentation process to find blood vessels in retinal images appropriately by a computer. It improved the performance of the segmentation method for detecting blood vessels in retinal image. Otsu Thresholding was used to segment blood vessel pixels and other pixels as background by local threshold. To evaluation performance of the proposed method, the study has been measured accuracy, sensitivity, and specificity. The DRIVE dataset's study results showed that the averages of accuracy, sensitivity, and specificity values were 94.7%, 72.28%, and 96.87%, respectively. It indicated that the proposed method was successful and well to work on blood vessels segmentation retinal images especially for thick blood vessels.



This is an open access article under the [CC-BY-SA](https://creativecommons.org/licenses/by-sa/4.0/) license.



1. Introduction

The retina is a crucial part on the human body. Diabetic Retinopathy (DR) is Changes in the structure of the eye's retina are a sign of a disease, such as Diabetic Retinopathy (DR) [1]. DR a change in the structure of the eye as a sign of someone having diabetes. It brings out abnormalities in the retinal blood vessels, results in blurry vision such as blurred vision and blindness [2]. Blood vessel abnormalities can be detected by segmenting blood vessels on retinal images generated by fundus cameras [3]. Blood vessel segmentation is typically performed by hand by experts/doctors. This process is time consuming

and disposed with human error, making it unsuitable for large amounts of image data and complicated blood vessel structures [4], [5]. As a result, automatic segmentation with the aid of a computer is required to obtain a more accurate and efficient segmentation of blood vessels.

Image quality has a significant impact on the retinal blood vessel segmentation result [1]. Retinal images produced by fundus cameras frequently have low contrast and noise, leading to misdiagnosis and the inability to detect disturbances [6]. Contrast Limited Adaptive Histogram Equalization or CLAHE is a technique to rise image contrast. The CLAHE method can be used uniformly to increase the image contrast and reduce noise on image [7], [8]. Several studies that used CLAHE to improve image contrast, including Shahid and Taj [4], Bahadar Khan, Khaliq and Shahid [5], and Ravichandran and Raja [9], produced good retinal blood vessel segmentation. Although the three studies reached accuracy and specificity levels above 95%, the resulting sensitivity value is still under 70%. Top-hat transformation is another method for increasing contrast. By increasing bright things from dark backgrounds, this method can highlight small objects with detail [10]. Several studies, including those conducted by Kushol *et al.* [11], Siddique *et al.* [12], and Bharkad [13], found that using the Top-hat transformation method after CLAHE resulted in better image quality, with the blood vessels in the retinal image being more precise and detailed than before. The accuracy and specificity obtained from the three studies were greater than 95%, but the sensitivity value obtained was still low under 75%.

Various segmentation methods have been developed, Otsu Thresholding is an efficient and easy segmentation method because the method uses local threshold values [7], [14]. Otsu Thresholding uses a different threshold at each pixel level that is in a partitioned sub-image of an image. Otsu Thresholding is a converting technique of RGB image into a binary image by determining the best threshold point. This method has the advantage of working better on enhanced images and performing simple computational calculations [15]. Several studies that have applied the Otsu Thresholding method for blood vessel segmentation include Tian *et al.* [7] used Otsu Thresholding with image improvement using Frangi Hessian and Improved mathematical morphology, resulting in accuracy and specificity of 95.54% and 98.02%, respectively, but the sensitivity value produced was still low at 69.42%. Ali and Muhammad [16] used Otsu Thresholding to improve the image using the Frangi filter, resulting in 96.99% accuracy and 97.28% specificity, but the sensitivity value remained low at 63.99%. Wang *et al.* [17] used Otsu Thresholding with a Hessian filter to improve the image, yielding a sensitivity value of 34.58% but did not discuss the accuracy and specificity results.

Several existing studies, they showed that image improvement greatly affected the results of segmentation on the image. This study used the combination technique and method for image enhancement and image segmentation. The study used CLAHE and Top-hat transformation in image enhancement. For segmentation, the proposed method used Otsu Thresholding. The Otsu thresholding used a different threshold at each pixel level that is in a partitioned sub-image of an image. On the study, Otsu thresholding involved many different threshold and calculated the size of the spreading for the pixel level on each side of the threshold. By using a local threshold on Otsu Thresholding, the results of segmentation between retinal blood vessel and background can be more accurate and valid because the threshold used is different for each sub-image of an retinal image. The expected result of this research was to obtain better and more accurate to get blood vessel segmentation on retinal image by Otsu Thresholding method through the stages of image quality enhancement.

2. Method

2.1. DRIVE Dataset

The dataset used for the study was the Digital Retinal Images for Vessel Extraction dataset (DRIVE), which can be downloaded for free from an online database <https://drive.grandchallenge.org/DRIVE/>. The DRIVE dataset has provided two groups of data, namely training data and testing data. Each group has provided as many as 20 images by DRIVE dataset. This dataset also included expert/doctoral analysis results that could be used as a baseline for comparing segmentation results. The images on DRIVE dataset had 565 x 584 pixels size with 96 dpi. The images were 712 KB in size, and saved in .tif format.

2.2. Image Enhancement

Image enhancement was the first step in image segmentation which aimed to remove noise, and increased image contrast to obtain a good segmentation result. The stages of image enhancement used in this study were:

2.2.1. Green Channel

First, a BGR retinal image was converted to an RGB image (Red, Green, Blue). Take a green channel that had less noise and a more stable contrast [1]. Compared to other RGB channels, the green channel could separate blood vessels and the background more clear than other channels [1], [18]. The Equation for the green channel could be found in Equation (1).

$$g(x, y) = \frac{G(x, y)}{R(x, y) + G(x, y) + B(x, y)} \quad (1)$$

where $g(x, y)$ was the green channel on image, $R(x, y)$ was red color intensity image pixel, $G(x, y)$ was green color intensity image pixel, and $B(x, y)$ was blue color intensity image pixel.

2.2.2. Complement Operation

A complement operation was performed to aid the clarification on blood vessels in retinal image [19]. The complement operation, also known as the negative image operation, improved the resulting image by subtracting each pixel from the maximum intensity value. Complement operations were computed by transforming functions with intensity levels ranging from $[0, L - 1]$. The Equation for the green channel could be found in Equation (2) [19].

$$T = S(t) = K - 1 - t \quad (2)$$

where $K - 1$ was the value of maximum intensity pixel with $K = 255$, T was the output of the new intensity pixel, and t was the input intensity value of green channel.

2.2.3. Contrast Limited Adaptive Histogram Equalization or CLAHE

CLAHE was used to enhance the image contrast. CLAHE is a method developed to forward the issue of low contrast and color unevenness on images, especially medical images [20]. The CLAHE worked by segmenting the image into contextual regions. After that, it applied Histogram Equalization (HE) for all area by flattening the gray color distribution. The process made hidden features in the image more seeable [21]. The CLAHE worked by assigning a limit value to the histogram and limiting contrast enhancement [22]. This limit value was known as the clip limit, and it specified the maximum height

of a histogram. To calculate the CLAHE result, it computed the average number of pixels in an image using Equation (3) [23].

$$M_{avg} = \frac{M_{CR-xp} - M_{CR-yp}}{M_{gray}} \quad (3)$$

where M_{avg} was the average pixels number, M_{gray} was a total of gray levels in the contextual region, M_{CR-xp} was the total pixels on the contextual region's x-axis, and M_{CR-yp} was the total pixels in the contextual region's y-axis. Furthermore, equation (4) was used to calculate the actual clip limit [24].

$$M_{CL} = M_{CLIP} \times M_{avg} \quad (4)$$

where M_{CL} was the actual clip limit value, and M_{CLIP} was the input CL in the range [0, 1].

2.2.4. Top-hat Transformation

The top-hat transformation was applied to give highlight on the retinal blood vessels in more detail. The Top-hat transformation is a redistributing technique of the grayscale intensity image to produce image characteristics. This technique could be used to highlight the structure of blood vessels while smoothing out the background [25]. Systematically, the Top-hat transformation equation could be seen in Equation (5) [25].

$$T_{hat}(A) = A \ominus (A \circ B) \quad (5)$$

where A represented the image input, B represented the structuring element or matrix operator, and \circ was operasi opening. This transformation aided in determining the overall shape of an object with varying intensities. The Top-hat transformation could highlight blood vessel structure while smoothing the background [25].

2.3. Segmentation

At this point, the image enhancement was transformed into a binary image by splitting the features in image into two parts, namely retinal blood vessels (foreground) as white pixels and not retinal blood vessels (background) as black pixels [26]. Otsu Thresholding was used in this study for retinal image segmentation. Thresholding functions worked to convert a gray image into a binary image. The process was dependent on the threshold value (U) to fix which areas were included into foreground and which areas were included into background. To create a binary image, the image binarization process was as followed [27]:

$$h(x, y) = \begin{cases} 1 & \text{jika } k(x, y) \geq U \\ 0 & \text{jika } k(x, y) < U \end{cases} \quad (6)$$

where $h(x, y)$ was the binary image of $k(x, y)$ function and U was the threshold point. In this study, Otsu Thresholding was used to automatically divide the gray histogram image into two different areas without requiring the user to enter a threshold value [15]. The threshold in this method referred to the threshold at the maximum variance. The following equations were used in the Otsu Thresholding method [28]: calculate the probability for the background pixel $r_1(t)$, the blood vessel pixel $r_2(t)$, the variance for the background pixel $\sigma_1^2(t)$, and the variance for blood vessel pixel $\sigma_2^2(t)$ using Equations (7) - (10) as followed [28]:

$$r_1(t) = \sum_{i=1}^t S(i) \quad (7)$$

$$r_2(t) = \sum_{i=t+1}^t S(i) \quad (8)$$

$$\sigma_1^2(t) = \sum_{i=1}^t S(i) [i - \mu_1(t)]^2 \left[\frac{S(i)}{r_1(t)} \right] \quad (9)$$

$$\sigma_2^2(t) = \sum_{i=t+1}^t S(i) [i - \mu_2(t)]^2 \left[\frac{S(i)}{r_2(t)} \right] \quad (10)$$

The average background pixels was $\mu_1(t)$ and blood vessel pixels $\mu_2(t)$ could be calculated using Equations (11) and (12) [28].

$$\mu_1(t) = \sum_{i=1}^t \left[\frac{i P(i)}{r_1(t)} \right] \quad (11)$$

$$\mu_2(t) = \sum_{i=1}^t \left[\frac{i P(i)}{r_2(t)} \right] \quad (12)$$

where t was the image's threshold value in the range $[0, K - 1]$. $S(i)$ was a probability for the i^{th} pixel defined as $S(i) = n(i)/n$, where $n(i)$ was number of total grayscale pixels and n was a number of total pixels. After that, it needed to calculate the variance between blood vessel pixels and background pixels using Equation (13) [28].

$$\sigma_w^2(t) = r_1(t) \sigma_1^2(t) + r_2(t) \sigma_2^2(t) \quad (13)$$

2.4. Evaluation

Several performance evaluation measures were applied to see the success of the study. The performances used were accuracy, sensitivity, and specificity. The accuracy was a metric to evaluate the success of the proposed method to segment retinal blood vessel and background on retinal image. A sensitivity was a measure of the proposed method's ability to predict retinal blood vessel pixels correctly. The specificity was a measure of the proposed method's ability to predict non-vessel pixels or background [9], [22]. The accuracy, sensitivity and specificity were measured by confusion matrix. Confusion Matrix was a table that contained 4 combinations of predicted results and actual results (Table 1) [29]. The true positive (TP) was a positive class that was guessed correctly. The False positive (FP) was a positive class that was guessed wrong. As well as true negative (TN) which was a negative class that was guessed right and false negative (FN) was a negative class that was guessed wrong. The accuracy, sensitivity and specificity could calculate by equation (14), equation (15) and equation (16) [30].

Table 1. Confusion matrix

Predicted Class	Actual Class	
	Positive	Negative
Positive	True Positif (TP)	False Positif (FP)
Negatif	False Negatif (FN)	True Negatif (TN)

$$accuracy = \frac{TP+TN}{TP+FP+TN+FN} \quad (14)$$

$$sensitivity = \frac{TP}{TP+FN} \quad (15)$$

$$specificity = \frac{TN}{TN+FP} \quad (16)$$

Overall, the steps proposed in this study was showed in Fig. 1. In Fig 1, image enhancement was carried out in 5 stages, namely green channel, top hat transformation, CLAHE and complement operation. green channel was used to take the green layer from the original image. The results at the image enhancement were used as input images at the segmentation stage. The method used in the segmentation stage was Otsu Thresholding. The results at the segmentation stage were compared with the ground truth that provided by the DRIVE dataset.

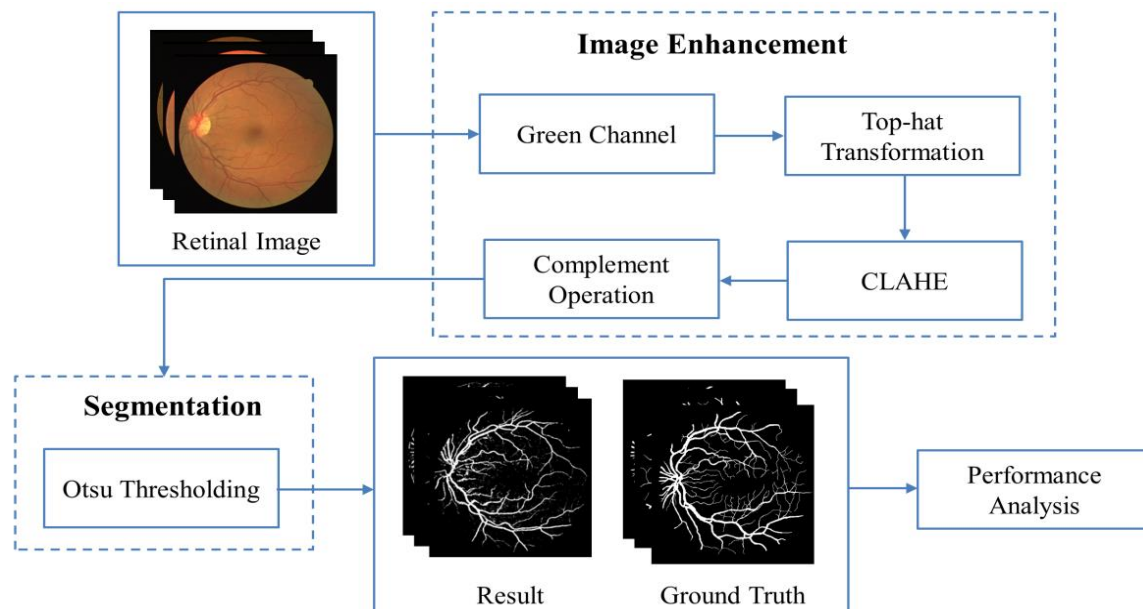


Fig. 1. Flowchart of blood vessels segmentation on proposed method

3. Results and Discussion

The result on training stage would be applied to 20 retinal images on testing data that provide by the DRIVE dataset. The testing data were processed in two stages: image enhancement and segmentation. The retinal image with BGR type was converted into RGB type during the image enhancement. Next, it took the green channel layer from the RGB image because it had a more stable contrast. The complement operation and CLAHE methods were then used to rise the contrast of the dark image. In the process, the image's detailed features could be seen clearly. Complement operation facilitated the separation of image objects from the background. The CLAHE repaired result still had noise, to smooth noise on image, the top-hat transformation was applied. The results of the top-hat transformation would be applied to segment using Otsu thresholds. It step was used to separate the features into two parts, namely the retinal blood vessels (foreground) as white pixels and the non-retinal blood vessels (background) as black pixels. The example results of images enhancement and segmentation on data testing could be seen in Fig. 2.

The histogram graph showed the success of increasing the contrast in an image. This graph described the frequency of occurrence of a pixel's intensity value. The comparisons of image histogram graphs between before CLAHE, after CLAHE, and Top-hat transformation were shown in Fig 3, Fig 4, and Fig 5.

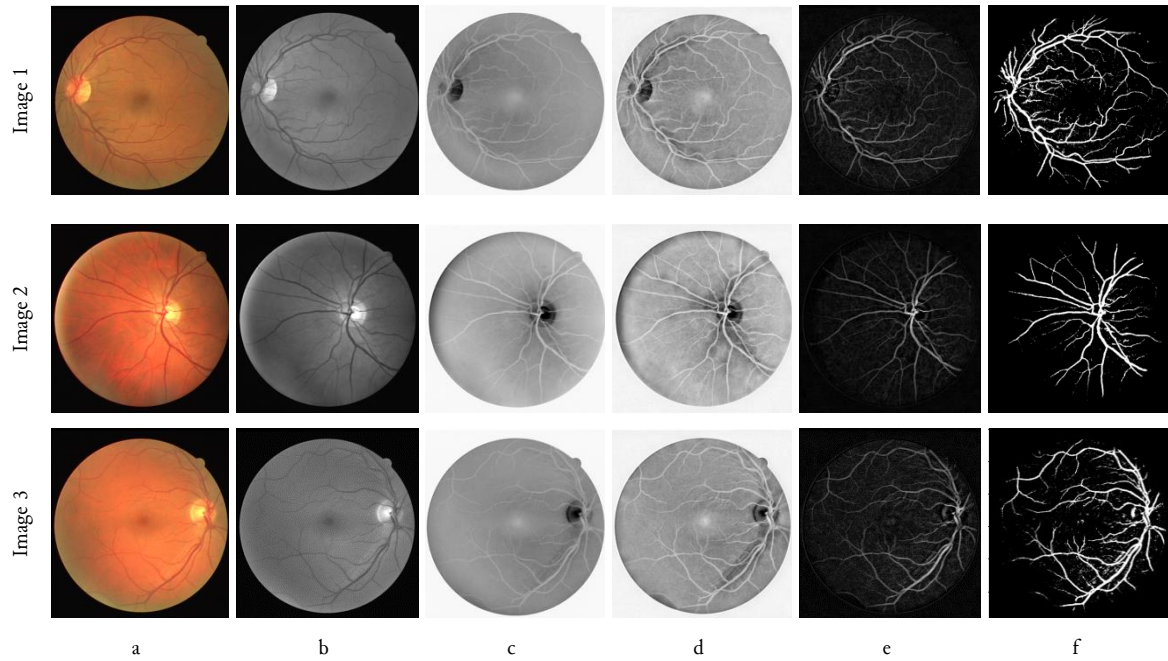


Fig. 2. The process of image enhancement and segmentation result (a) RGB (b) Green channel (c) Complement operation (d) CLAHE (e) Top-hat transformation (f) Otsu Thresholding

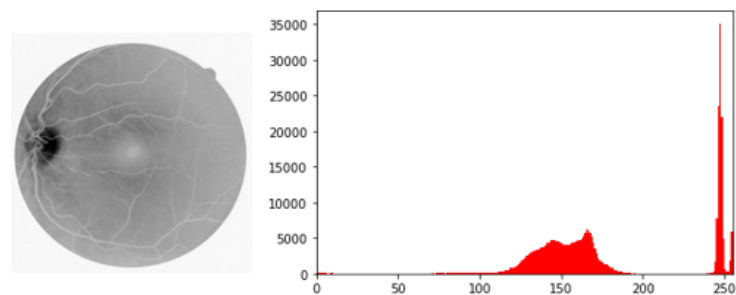


Fig. 3. Histogram graph of before CLAHE

According to the distribution of the histogram graph of the image before CLAHE in Fig. 3, the graph appeared irregular. It had an uneven height or frequency of pixel values. Visually, the pattern of blood vessels in the image before CLAHE was not visible due to the varying contrast of the image, so it was necessary to rise the contrast and degrade the brightness of the image.

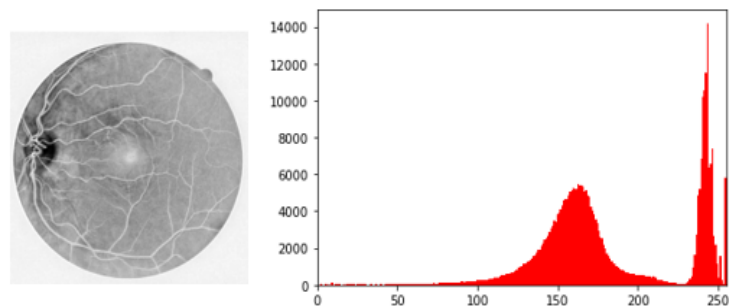


Fig. 4. Histogram graph of after CLAHE

On Fig. 4, it showed that the resulting image after CLAHE had better contrast quality than the image in Fig. 3. In the graph of the histogram equalization results, it could be seen that the frequency of occurrence of pixel values or the height of the graph were more evenly distributed compared to the previous image. Image pixel values after CLAHE spread in the range 0 to 255.

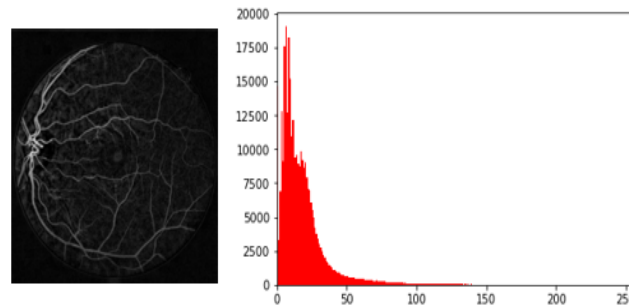


Fig. 5. Histogram graph of top-hat transformation.

In Fig. 5, it could be seen that a dark black color dominates the image resulting from the Top-hat transformation in the histogram graph. This could be seen in the distribution of pixel values, which tend to approach 0 with a range of 0 to 140. Even though the image was dark, the retinal blood vessel pattern was more visible in general. Table 2 showed the examples of the prediction results of retinal blood vessel segmentation and ground truth for 10 testing data.

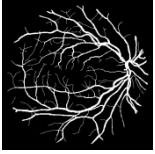
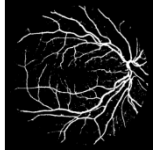
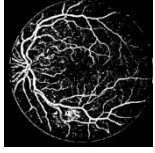
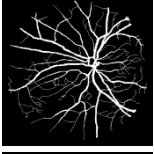
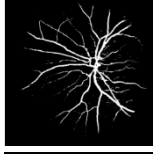
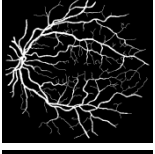
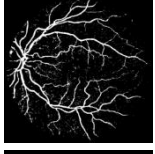
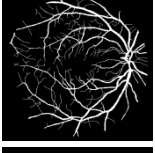
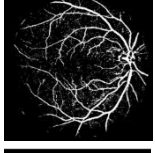
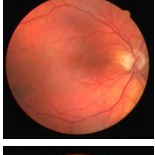
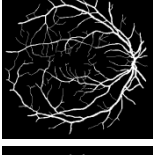
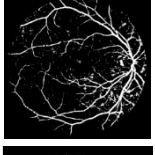
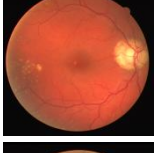
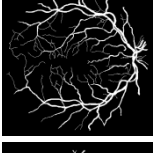
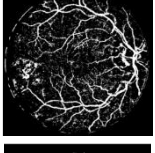
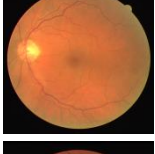
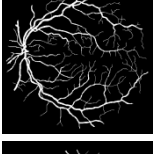
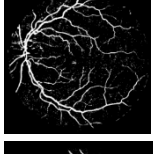
The proposed method worked in retinal blood vessels segmentation in images. In Table 2, it compared to each image's ground truth. However, there were still some thin blood vessels that cannot be properly segmented. Each pixel in each image was 565 x 584 pixels. Total pixels of all image in segmentation prediction result would be included in a confusion matrix. Confusion matrix was applied to calculate accuracy, sensitivity, and specificity for the proposed method [31], [32]. The confusion matrix obtained by the blood vessel segmentation process was displayed in Table 3.

According to Table 3, the TP value was 417801, which indicates that the total number pixels of retinal blood vessels that were correctly predicted in the segmentation results was 417801 pixels. Furthermore, the FP value was 195621, implying there were 195621 background pixels which were predicted as retinal blood vessels in the segmentation results. Then, the FN value was 160144 pixels, indicating that the number of retinal blood vessels predicted as background in the segmentation results was 160144 pixels. Then, the TN value was 5825634, indicating that the total pixels number that were correctly predicted as the background was 5825634 pixels in segmentation results. Based on Table 2, it could calculate the accuracy, sensitivity and specificity to evaluate the segmentation result that obtained from the proposed method on this study. Table 4 was the performance results of the 20 testing data.

Table 2. The Confusion Matrix result of the proposed method for retinal blood vessels segmentation

<i>Ground truth</i>	<i>Segmentation Result</i>	
	<i>Blood vessels</i>	<i>Background</i>
Blood vessels	417801	160144
Background	195621	5825634

Table 3. The Comparison of 10 segmentation testing images of results on proposed method with ground truth images by DRIVE dataset

No	Original Image	Segmentation	
		Ground Truth	Result
1			
2			
3			
4			
5			
6			
7			
8			
9			
10			

The high accuracy result was not enough to conclude the method was good or not. An accuracy only counted the total number of correct predictions regardless of the proportion of each class. Sensitivity and specificity measure label prediction correctly based on each class. High accuracy can be said to be good in predicting the majority class but not for the minority class. Therefore other measurements were needed, namely sensitivity to measure the success of the proposed method in detecting blood vessels and specificity to measure the success of the method in detecting the background in an image.

Table 4. Measurement Results for Accuracy, Sensitivity, and Specificity

Image No	Accuracy (%)	Sensitivity (%)	Specificity (%)
1	95.9	77.11	97.74
2	96.04	72.3	98.75
3	92.42	75.35	94.31
4	95.64	57.31	99.53
5	95.13	66.42	98.1
6	94.02	70.41	96.56
7	94.56	66.96	97.33
8	91.42	75.2	92.94
9	95.43	67.6	97.89
10	95.13	70.02	97.38
11	95.47	63.07	98.66
12	92.51	79.48	93.74
13	94.96	67.08	97.98
14	93.91	80.57	95.08
15	94.64	74.36	96.2
16	95.84	69.85	98.42
17	94.71	71.85	96.82
18	95.37	74.54	97.16
19	95.9	86.16	96.79
20	94.91	79.95	96.1

The sensitivity in Table 4 was smaller than the results of accuracy and specificity. Sensitivity was measured the machine performance in detecting retinal blood vessels. The retinal image consist of thick blood vessels and thin blood vessels. The thin blood vessels in the retina were more numerous than the retinal blood vessels. In addition, the thin retinal blood vessels were sometimes not well visible on retinal images. In contrast to sensitivity, specificity actually measured the success of the computer in detecting the background in the image. Background detection was easier because It only needs to remove the unused part. The condition of some very thin retinal blood vessels could cause the machine to be unable to detect these blood vessels. It caused the sensitivity results for each image in Table 4 were lower than their accuracy and specificity. The averages of accuracy, sensitivity, and specificity result of the study for 20 DRIVE testing data were 94.7%, 72.28%, and 96.87%, respectively, according to Table 4. The image number 2 obtained the highest accuracy value of 96.04%, where the segmented prediction results in the image almost resembled with ground truth. In contrast, the image number 8 obtained the lowest

accuracy value of 91.42% because the segmentation prediction results still had a lot of noise. The sensitivity of image number 19 was 86.16%. It showed the highest sensitivity result. It indicated that thin blood vessels could be detected properly by proposed method. For image number 8, it had the lowest sensitivity value of 57.31% because the predicted image could not detect thin blood vessels on the image.

The highest specificity result obtained by image number 4 of 99.53%. From the Table 4, the segmented image still had little noise compared with ground truth image, and the lowest specificity value obtained by image number 8 of 92.94%. It meant the predicted image still had a lot of noise it could be seen also on Table 4. Overall, the accuracy, sensitivity, and specificity of the proposed method for retinal blood vessels segmentation were considered high and could help the medical team to diagnose retinal blood vessels. However, there were still thin blood vessels that could not be detected and segmented visually. It meant the proposed method was still needed improvement to detect thin blood vessel on retinal images.

Table 5. The comparison results study on blood vessels segmentation in retinal image

Method	Result		
	Accuracy (%)	Sensitivity (%)	Specificity
Frangi hessian + Otsu Thresholding [7]	95.54	69.42	98.02
Top-hat and Bottom-hat Transform + RUSBoost Classifier [11]	93.79	62.96	98.30
Frangi filter + Otsu Thresholding [16]	96.99	63.99	97.28
Hessian based linear filter + Otsu thresholding [17]	-	34.58	-
CLAHE-Average Filter + Isodata Thresholding [33]	94.78	43.46	98.81
Adaptive matched filter [34]	93.7	72.05	95.79
Proposed Method (DRIVE)	94.7	72.28	96.87

According to Table 5, Ali and Muhammad [16] achieved the highest accuracy value of 96.99% by combining Otsu Thresholding with image improvement using the Frangi filter. However, the sensitivity value was lower than that of the proposed method and research by Tian *et al.* [7]. The proposed method yielded the highest sensitivity value of 72.28%. Erwin and Damayanti [33] achieved the highest specificity value of 98.81% using Isodata thresholding with image enhancement using CLAHE and Average Filter, but the sensitivity produced was still low 43.46%. From the average performance of proposed method results, it could be concluded that the accuracy of architecture for segmenting blood vessels was excellent, as indicated by an accuracy value of 94.7%. The sensitivity value of 72.28% was also quite good to predict retinal compared to other studies. Based on sensitivity value, the proposed method works well on thick blood vessels on retinal image but it still needs to improve the method to predict on thin retinal blood vessels. With a specificity value of 0.961, the proposed method on the study has an excellent ability to predict background pixels on retinal image.

4. Conclusion

According to the results of previous research, the proposed method using the Otsu Thresholding combining with image enhancement. The image enhancement used CLAHE and Top-hat transformation. The proposed method can work well in blood vessels segmentation in retinal image with the average accuracy was 94.7%, sensitivity was 72.28%, and specificity was 96.87%. These results meant the proposed method was well to segment and separate the blood vessels and the background on retinal image. The segmentation results also demonstrated that the blood vessels were successfully extracted visually especially for thick vessel. The sensitivity was 72.28%. It showed the proposed method is good to segment thick blood vessel on retinal image but it should be improved to segment the thin blood vessel of retina to increase the sensitivity performance on blood vessel segmentation on retinal image. Based on the specificity value, the proposed method is excellent to segment or predict pixels background on retinal images.

Acknowledgment

Thank to DRIVE project team for making their image database publicly available on the Internet and To Sriwijaya University (UNSRI) that provided facility for this study.

Declarations

Author contribution. All authors contributed equally to the main contributor to this paper. All authors read and approved the final paper.

Funding statement. None of the authors have received any funding or grants from any institution or funding body for the research.

Conflict of interest. The authors declare no conflict of interest.

Additional information. No additional information is available for this paper.

References

- [1] T. A. Soomro *et al.*, "Impact of Novel Image Preprocessing Techniques on Retinal Vessel Segmentation," *Electronics*, vol. 10, no. 18, pp. 1–19, Sep. 2021, doi: [10.3390/electronics10182297](https://doi.org/10.3390/electronics10182297).
- [2] S. Gayathri, V. P. Gopi, and P. Palanisamy, "Automated classification of diabetic retinopathy through reliable feature selection," *Phys. Eng. Sci. Med.*, vol. 43, no. 3, pp. 927–945, Sep. 2020, doi: [10.1007/s13246-020-00890-3](https://doi.org/10.1007/s13246-020-00890-3).
- [3] R. Rajalakshmi, V. Prathiba, S. Arulmalar, and M. Usha, "Review of retinal cameras for global coverage of diabetic retinopathy screening," *Eye*, vol. 35, no. 1, pp. 162–172, Jan. 2021, doi: [10.1038/s41433-020-01262-7](https://doi.org/10.1038/s41433-020-01262-7).
- [4] M. Shahid and I. A. Taj, "Retracted: Robust Retinal Vessel Segmentation using Vessel's Location Map and Frangi Enhancement Filter," *IET Image Process.*, vol. 12, no. 4, pp. 494–501, Apr. 2018, doi: [10.1049/iet-ipr.2017.0457](https://doi.org/10.1049/iet-ipr.2017.0457).
- [5] K. BahadarKhan, A. A Khaliq, and M. Shahid, "A Morphological Hessian Based Approach for Retinal Blood Vessels Segmentation and Denoising Using Region Based Otsu Thresholding," *PLoS One*, vol. 11, no. 7, pp. 1–19, Jul. 2016, doi: [10.1371/journal.pone.0158996](https://doi.org/10.1371/journal.pone.0158996).
- [6] Z. Shen, H. Fu, J. Shen, and L. Shao, "Modeling and Enhancing Low-Quality Retinal Fundus Images," *IEEE Trans. Med. Imaging*, vol. 40, no. 3, pp. 996–1006, Mar. 2021, doi: [10.1109/TMI.2020.3043495](https://doi.org/10.1109/TMI.2020.3043495).

- [7] F. Tian, Y. Li, J. Wang, and W. Chen, "Blood Vessel Segmentation of Fundus Retinal Images Based on Improved Frangi and Mathematical Morphology," *Comput. Math. Methods Med.*, vol. 2021, pp. 1–11, May 2021, doi: [10.1155/2021/4761517](https://doi.org/10.1155/2021/4761517).
- [8] J. Ma, X. Fan, S. X. Yang, X. Zhang, and X. Zhu, "Contrast Limited Adaptive Histogram Equalization-Based Fusion in YIQ and HSI Color Spaces for Underwater Image Enhancement," *Int. J. Pattern Recognit. Artif. Intell.*, vol. 32, no. 07, p. 1854018, Jul. 2018, doi: [10.1142/S0218001418540186](https://doi.org/10.1142/S0218001418540186).
- [9] C. G. Ravichandran and J. B. Raja, "A Fast Enhancement/Thresholding Based Blood Vessel Segmentation for Retinal Image Using Contrast Limited Adaptive Histogram Equalization," *J. Med. Imaging Heal. Informatics*, vol. 4, no. 4, pp. 567–575, Aug. 2014, doi: [10.1166/jmih.2014.1289](https://doi.org/10.1166/jmih.2014.1289).
- [10] O. Ramos-Soto *et al.*, "An efficient retinal blood vessel segmentation in eye fundus images by using optimized top-hat and homomorphic filtering," *Comput. Methods Programs Biomed.*, vol. 201, pp. 1–13, Apr. 2021, doi: [10.1016/j.cmpb.2021.105949](https://doi.org/10.1016/j.cmpb.2021.105949).
- [11] R. Kushol, M. H. Kabir, M. S. Salekin, and A. B. M. A. Rahman, "Contrast Enhancement by Top-Hat and Bottom-Hat Transform with Optimal Structuring Element: Application to Retinal Vessel Segmentation," in *Lecture Notes in Computer Science (including subseries Lecture Notes in Artificial Intelligence and Lecture Notes in Bioinformatics)*, vol. 10317, 2017, pp. 533–540. doi: [10.1007/978-3-319-59876-5_59](https://doi.org/10.1007/978-3-319-59876-5_59)
- [12] F. Siddique, T. Iqbal, S. M. Awan, Z. Mahmood, and G. Z. Khan, "A Robust Segmentation of Blood Vessels in Retinal Images," in *2019 International Conference on Frontiers of Information Technology (FIT)*, 2019, pp. 83–835, doi: [10.1109/FIT47737.2019.00025](https://doi.org/10.1109/FIT47737.2019.00025).
- [13] S. Bharkad, "Automatic segmentation of blood vessels in retinal image using morphological filters," in *Proceedings of the 6th International Conference on Software and Computer Applications - ICSCA '17*, 2017, pp. 132–136, doi: [10.1145/3056662.3056710](https://doi.org/10.1145/3056662.3056710).
- [14] E. Erwin, S. Saparudin, and W. Saputri, "Hybrid multilevel thresholding and improved harmony search algorithm for segmentation," *Int. J. Electr. Comput. Eng.*, vol. 8, no. 6, pp. 4593–4602, 2018, doi: [10.11591/ijece.v8i6.pp4593-4602](https://doi.org/10.11591/ijece.v8i6.pp4593-4602).
- [15] F. Bukenya, L. Bai, and A. Kiweewa, "A Review of Blood Vessel Segmentation Techniques," in *2018 1st International Conference on Computer Applications & Information Security (ICCAIS)*, 2018, pp. 1–10, doi: [10.1109/CAIS.2018.8441989](https://doi.org/10.1109/CAIS.2018.8441989).
- [16] O. Ali, N. Muhammad, Z. Jadoon, B. M. Kazmi, N. Muzamil, and Z. Mahmood, "A Comparative Study of Automatic Vessel Segmentation Algorithms," in *2020 3rd International Conference on Computing, Mathematics and Engineering Technologies (iCoMET)*, 2020, pp. 1–6, doi: [10.1109/iCoMET48670.2020.9074073](https://doi.org/10.1109/iCoMET48670.2020.9074073).
- [17] H. Wang, Y. Jiang, X. Jiang, J. Wu, and X. Yang, "Automatic vessel segmentation on fundus images using vessel filtering and fuzzy entropy," *Soft Comput.*, vol. 22, no. 5, pp. 1501–1509, Mar. 2018, doi: [10.1007/s00500-017-2872-4](https://doi.org/10.1007/s00500-017-2872-4).
- [18] K. B. Shaik, P. Ganesan, V. Kalist, B. S. Sathish, and J. M. M. Jenitha, "Comparative Study of Skin Color Detection and Segmentation in HSV and YCbCr Color Space," *Procedia Comput. Sci.*, vol. 57, pp. 41–48, 2015, doi: [10.1016/j.procs.2015.07.362](https://doi.org/10.1016/j.procs.2015.07.362).
- [19] H. A. Nugroho, T. Lestari, R. A. Aras, and I. Ardiyanto, "Segmentation of retinal blood vessels using Gabor wavelet and morphological reconstruction," in *2017 3rd International Conference on Science in Information Technology (ICSITech)*, 2017, pp. 513–516, doi: [10.1109/ICSITech.2017.8257166](https://doi.org/10.1109/ICSITech.2017.8257166).
- [20] A. Desiani, B. Suprihatin, S. Yahdin, A. I. Putri, and F. R. Husein, "Bi-path architecture of CNN segmentation and classification method for cervical cancer disorders based on pap-smear images," *IAENG Int. J. Comput. Sci.*, vol. 48, no. 3, pp. 782–791, 2021. Available at: [Google Scholar](https://www.google.com/scholar).
- [21] Sonali, S. Sahu, A. K. Singh, S. P. Ghrera, and M. Elhoseny, "An approach for de-noising and contrast enhancement of retinal fundus image using CLAHE," *Opt. Laser Technol.*, vol. 110, pp. 87–98, Feb. 2019, doi: [10.1016/j.optlastec.2018.06.061](https://doi.org/10.1016/j.optlastec.2018.06.061).
- [22] P. Singh, R. Mukundan, and R. De Ryke, "Feature Enhancement in Medical Ultrasound Videos Using Contrast-Limited Adaptive Histogram Equalization," *J. Digit. Imaging*, vol. 33, no. 1, pp. 273–285, Feb. 2020, doi: [10.1007/s10278-019-00211-5](https://doi.org/10.1007/s10278-019-00211-5).

- [23] Y. Chang, C. Jung, P. Ke, H. Song, and J. Hwang, "Automatic Contrast-Limited Adaptive Histogram Equalization With Dual Gamma Correction," *IEEE Access*, vol. 6, pp. 11782–11792, 2018, doi: [10.1109/ACCESS.2018.2797872](https://doi.org/10.1109/ACCESS.2018.2797872).
- [24] S. H. Majeed and N. A. M. Isa, "Iterated Adaptive Entropy-Clip Limit Histogram Equalization for Poor Contrast Images," *IEEE Access*, vol. 8, pp. 144218–144245, 2020, doi: [10.1109/ACCESS.2020.3014453](https://doi.org/10.1109/ACCESS.2020.3014453).
- [25] Z. Jiang, J. Yopez, S. An, and S. Ko, "Fast, accurate and robust retinal vessel segmentation system," *Biocybern. Biomed. Eng.*, vol. 37, no. 3, pp. 412–421, 2017, doi: [10.1016/j.bbe.2017.04.001](https://doi.org/10.1016/j.bbe.2017.04.001).
- [26] S. Pal, S. Chatterjee, D. Dey, and S. Munshi, "Morphological operations with iterative rotation of structuring elements for segmentation of retinal vessel structures," *Multidimens. Syst. Signal Process.*, vol. 30, no. 1, pp. 373–389, Jan. 2019, doi: [10.1007/s11045-018-0561-9](https://doi.org/10.1007/s11045-018-0561-9).
- [27] K. Kipli *et al.*, "Morphological and Otsu's Thresholding-Based Retinal Blood Vessel Segmentation for Detection of Retinopathy," *Int. J. Eng. Technol.*, vol. 7, no. 3.18, p. 16, Aug. 2018, doi: [10.14419/ijet.v7i3.18.16665](https://doi.org/10.14419/ijet.v7i3.18.16665).
- [28] W. - and Y. Palgunadi, "Blood Vessels Segmentation in Retinal Fundus Image using Hybrid Method of Frangi Filter, Otsu Thresholding and Morphology," *Int. J. Adv. Comput. Sci. Appl.*, vol. 10, no. 6, pp. 417–422, 2019, doi: [10.14569/IJACSA.2019.0100654](https://doi.org/10.14569/IJACSA.2019.0100654).
- [29] F. Krüger, "Activity, Context, and Plan Recognition with Computational Causal Behaviour Models," University of Rostock, 2016. Available at: [Google Scholar](https://scholar.google.com/).
- [30] S. Yahdin, A. Desiani, A. Amran, D. Rodiah, and Solehan, "Pattern recognition for study period of student in Mathematics Department with C4.5 algorithm data mining technique at the Faculty of Mathematics and Natural Science Universitas Sriwijaya," *J. Phys. Conf. Ser.*, vol. 1282, no. 1, pp. 1–6, Jul. 2019, doi: [10.1088/1742-6596/1282/1/012014](https://doi.org/10.1088/1742-6596/1282/1/012014).
- [31] A. Desiani, N. R. Dewi, A. N. Fauza, N. Rachmatullah, M. Arhami, and M. Nawawi, "Handling Missing Data Using Combination of Deletion Technique, Mean, Mode and Artificial Neural Network Imputation for Heart Disease Dataset," *Sci. Technol. Indones.*, vol. 6, no. 4, pp. 303–312, Oct. 2021, doi: [10.26554/sti.2021.6.4.303-312](https://doi.org/10.26554/sti.2021.6.4.303-312).
- [32] A. Desiani, S. Yahdin, A. Kartikasari, and I. Irmeilyana, "Handling the imbalanced data with missing value elimination SMOTE in the classification of the relevance education background with graduates employment," *IAES Int. J. Artif. Intell.*, vol. 10, no. 2, pp. 346–354, Jun. 2021, doi: [10.11591/ijai.v10.i2.pp346-354](https://doi.org/10.11591/ijai.v10.i2.pp346-354).
- [33] Erwin and H. R. Damayanti, "Supervised Retinal Vessel Segmentation Based Average Filter and Iterative Self Organizing Data Analysis Technique," *Int. J. Comput. Intell. Appl.*, vol. 20, no. 01, pp. 1–13, Mar. 2021, doi: [10.1142/S1469026821500036](https://doi.org/10.1142/S1469026821500036).
- [34] T. Chakraborti, D. K. Jha, A. S. Chowdhury, and X. Jiang, "A self-adaptive matched filter for retinal blood vessel detection," *Mach. Vis. Appl.*, vol. 26, no. 1, pp. 55–68, Jan. 2015, doi: [10.1007/s00138-014-0636-z](https://doi.org/10.1007/s00138-014-0636-z).